Nucleic Acids Research, 2023, 1–16
https://doi.org/10.1093/nar/gkad825
Gene regulation, Chromatin and Epigenetics

OXFORD

Different elongation factors distinctly modulate RNA polymerase II transcription in Arabidopsis

Simon Obermeyer [1], Lukas Schrettenbrunner[1], Richard Stöckl[1], Uwe Schwartz[2] and Klaus D. Grasser [1,*]

[1]Cell Biology & Plant Biochemistry, Biochemistry Centre, University of Regensburg, Universitätsstr. 31, D-93053 Regensburg, Germany
[2]NGS Analysis Centre, Biology and Pre-Clinical Medicine, University of Regensburg, Universitätsstr. 31, D-93053 Regensburg, Germany
[*]To whom correspondence should be addressed. Tel: +49 941 9433032; Fax: +49 941 9433352; Email: Klaus.Grasser@ur.de

Abstract

Various transcript elongation factors (TEFs) including modulators of RNA polymerase II (RNAPII) activity and histone chaperones tune the efficiency of transcription in the chromatin context. TEFs are involved in establishing gene expression patterns during growth and development in *Arabidopsis*, while little is known about the genomic distribution of the TEFs and the way they facilitate transcription. We have mapped the genome-wide occupancy of the elongation factors SPT4–SPT5, PAF1C and FACT, relative to that of elongating RNAPII phosphorylated at residues S2/S5 within the carboxyterminal domain. The distribution of SPT4–SPT5 along transcribed regions closely resembles that of RNAPII-S2P, while the occupancy of FACT and PAF1C is rather related to that of RNAPII-S5P. Under transcriptionally challenging heat stress conditions, mutant plants lacking the corresponding TEFs are differentially impaired in transcript synthesis. Strikingly, in plants deficient in PAF1C, defects in transcription across intron/exon borders are observed that are cumulative along transcribed regions. Upstream of transcriptional start sites, the presence of FACT correlates with nucleosomal occupancy. Under stress conditions FACT is particularly required for transcriptional upregulation and to promote RNAPII transcription through +1 nucleosomes. Thus, *Arabidopsis* TEFs are differently distributed along transcribed regions, and are distinctly required during transcript elongation especially upon transcriptional reprogramming.

Graphical abstract

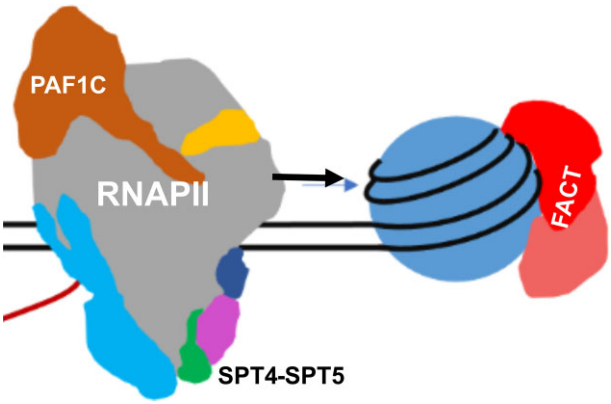

Introduction

Protein-coding genes are transcribed by RNA polymerase II (RNAPII), which plays a fundamental role in differential gene expression to ensure that appropriate amounts of mRNAs are produced in a spatially and temporally coordinated manner. Proper mRNA synthesis is an essential prerequisite for growth, development and response to environmental conditions. RNAPII transcription is characterised by a cycle of events including initiation, elongation and termination, and in addition to controlling the initiation step, the efficiency of mRNA production is regulated during elongation (1,2). Throughout the transcription cycle, the carboxyterminal domain (CTD) of the largest subunit of RNAPII is dynamically phosphorylated within its heptapeptide repeats including S2P and S5P, which are characteristic of the elongating polymerase (3,4). In the cell nucleus, the DNA template for transcription is wrapped around histone octamers, forming nucleosomes that represent obstacles for RNAPII progression. Consequently, the elongation phase of transcription on chromatin templates is a dynamic and discontinuous process (5,6). Studies primarily in yeast and mammals demonstrated that transcriptional elongation (and its coordination with co-transcriptional events) is promoted by a variety of transcript elongation factors (TEFs) to assist mRNA synthesis by RNAPII. TEFs serve

Received: April 14, 2023. **Revised:** August 24, 2023. **Editorial Decision:** September 18, 2023. **Accepted:** September 21, 2023

diverse functions including modulating the catalytic properties and processivity of RNAPII and relieving progression of the enzyme through repressive chromatin (2,7–9). During the past few years, advances in cryo-electron microscopy in combination with X-ray crystallography allowed elucidation of many details regarding the three-dimensional organisation of elongating RNAPII associated with various TEFs (9–11).

The heterodimeric TEF, SPT4–SPT5, is conserved in eukaryotes and archaea and associates with RNAPII in a transcription-dependent manner (12). SPT4–SPT5 is involved in various aspects of transcript elongation including stabilisation of the RNAPII elongation complex, transcription through nucleosomes, regulation of RNAPII pausing, as well as transcriptional termination and the coordination with co-transcriptional mRNA processing (13,14). The multifunctional TEF, PAF1C, in higher eukaryotes consists of six subunits and associates with RNAPII to stabilise the elongation complex and to promote transcription (15,16). Furthermore, PAF1C links transcript elongation with post-translational histone modifications along actively transcribed regions, including H2B mono-ubiquitination and various histone methylations (i.e. H3K4me2/3, H3K36me3, K3K79me2/3). Therefore, as a global regulatory factor PAF1C functions at the interface between chromatin and transcription (15,16). Another factor that is considered to be a TEF is the FACT histone chaperone consisting of the SSRP1 and SPT16 subunits. FACT can facilitate disassembly and reassembly of nucleosomes, thus it is effective in various DNA-dependent processes such as replication, repair and transcription (17,18). The reversible nucleosome reorganisation is accomplished by multiple contacts of the FACT subunits with histones and the nucleosomal DNA. During elongation FACT promotes transcription of RNAPII through nucleosomes, but importantly it also assists reassembly of nucleosomes after RNAPII passage (17–19).

A number of studies, particularly in the *Arabidopsis thaliana* model, have revealed that various TEFs play vital roles in governing plant growth and development (20,21). In *Arabidopsis*, each subunit of SPT4–SPT5 is encoded by two genes and the ubiquitously expressed *SPT5-2* proved essential. SPT4-RNAi plants expressing reduced amounts of *SPT4* (and SPT5–2) exhibit growth and developmental defects of which some may be caused by inadequate auxin signalling (22). Moreover, SPT4–SPT5 modulates plant thermomorphogenesis and salt tolerance (23,24). Along with other TEFs, SPT4–SPT5 associate with elongating RNAPII, forming the active elongation complex (22,25). *Arabidopsis* PAF1C consisting (as in mammals) of six subunits associates with RNAPII (25) and was initially recognised because of its role in the transition from vegetative to reproductive development. The early flowering phenotype of plants deficient in PAF1C subunits is associated with reduced expression of the floral repressor *FLC* (26–30). In addition, PAF1C proved to be involved in plant response to mechanical stimulation inflicted by repeated touch (31) as well as in the response to elevated salt concentration (32,33). The FACT histone chaperone composed of SSRP1 and SPT16 associates with transcribed regions of *Arabidopsis* genes in a transcription-dependent manner (25,34,35). FACT proved essential for viability (36,37) and decreased *SSRP1/SPT16* expression levels resulted in a variety of vegetative and reproductive defects including increased number of leaves, early bolting, reduced seed set and impaired circadian rhythm (37,38). Moreover, FACT is critically involved in the repression of aberrant transcript initiation from within coding regions of RNAPII-transcribed genes (39).

While substantial information has been gathered about the role of TEFs in plant development, knowledge regarding genome-wide impact of TEF function on RNAPII transcription as well as their contribution to (rapid) transcriptional reprogramming is rather incomplete. Therefore, we have comparatively analysed three types of *Arabidopsis* TEF (SPT4–SPT5, PAF1C and FACT) regarding their genomic distribution relative to elongating RNAPII. In addition, their involvement in the transcriptional response to challenging conditions was examined by analysing corresponding mutant plants relative to wildtype. The comparative analysis uncovered that the three types of TEFs distinctly influence transcript elongation in the context of plant chromatin.

Materials and methods

Plant material

Seeds of *Arabidopsis thaliana* Col-0 were sown on solid 0.5x MS medium (40) and after stratification for 48h at 4°C in the dark, the plates were transferred to a plant incubator (PolyKlima) with long day settings with 16h light (110 $\mu mol \cdot m^{-2} \cdot s^{-1}$) at 21°C and 8h darkness at 18°C. For heat stress treatment the plates were transferred to a water bath set to 44°C for 10 min (41) and snap frozen in liquid nitrogen, as previously described (42). Plant lines used in this study were described before: *ssrp1-2 (*SALK_001283), *spt16-1* (SAIL_392_G06) (37), *elf7-3* (SALK_019433) (26) and SPT4-RNAi line 3 (termed *SPT4-R3*) (22).

Chromatin Immunoprecipitation

Chromatin immunoprecipitation (ChIP) was essentially performed as described previously (43,44). *Arabidopsis* plants grown *in vitro* (14 days after stratification, 14-DAS) were crosslinked with formaldehyde and used for isolation of nuclei, before chromatin was sheared using a Bioruptor Pico device (Diagenode, Seraing, Belgium). Immunoprecipitation was carried out using magnetic Dynabeads Protein A (Thermo Fisher Scientific). Elongation factor ChIPs were performed with previously described antibodies directed against purified, recombinant domains of elongation factors SPT5-2 (aaT792-P1041) (22), ELF7 (aaD401-E589) (25), SSRP1 (aaV453-N646) and SPT16 (aaE416-M554) (34). RNAPII ChIPs were performed with antibodies against RNAPII-S2P (ab5095; Abcam) and RNAPII-S5P (ab5131; Abcam).

Chromatin immunoprecipitation sequencing (ChIP-seq)

Libraries were prepared using the NEBnext UltraII Library preparation kit with 6bp NEBNext Multiplex Oligonucleotides for Illumina according to the manufacturer with minor modifications. ChIP-seq was carried out as described in the Illumina NextSeq 500 System Guide (Illumina), and the KAPA Library Quantification Kit - Illumina/ABI Prism (Roche Sequencing Solutions). Equimolar amounts of each library were sequenced on a NextSeq 500 instrument controlled by the NextSeq Control Software (NCS) v2.2.0, using the 75 Cycles High Output Kit with single index, single-read (SR) run parameters. Image analysis and base calling were done by the Real Time Analysis Software (RTA) v2.4.11. The resulting .bcl files were converted into .fastq files with

the bcl2fastq v2.18 software. ChIPseq was performed at the Genomics Core Facility 'KFB - Center of Excellence for Fluorescent Bioanalytics' (University of Regensburg, Regensburg, Germany; www.kfb-regensburg.de). Sequencing resulted in an average of 17.7M reads per library (min 12.8M, max 23.9M) with an average Phred score >34 (Table S1).

ChIP-seq data analysis

Reads were trimmed using Trimmomatic (v0.39) (45) followed by alignment to the TAIR10 genome (https://www.arabidopsis.org/) using Bowtie2 (46) using the preset mode *–local –very-sensitive-local*. Alignment files were converted to .bam files containing only alignments with MAPQ score > 10, sorted and indexed using the samtools suite (v1.16.1) (47). Coverage tracks were calculated using deepTools 'bamCoverage'. Downstream analysis was mainly performed using the deepTools2 suite (v.3.5.0) (48). Quality control was performed at several steps using FastQC (https://www.bioinformatics.babraham.ac.uk/projects/fastqc/). Genomic regions with aberrant coverage or low sequence complexity were filtered out, as described previously (49). After confirming high pairwise correlations and performing hierarchical clustering analysis (Supplementary Figures S1, S2), the biological replicates (four replicates for SPT5, ELF7, SSRP1 and SPT16 and two replicates for RNAPII-S2P and -S5P) were merged and CPM normalised. Peaks were called using the MACS3 (50) *callpeak* function with RNAPII-S2P and RNAPII-S5P as control, respectively, with the following arguments *-g 119 481 543 -B -q 0.01 –nomodel*.

MNase-seq data analysis

Analyses were performed as previously described (42) and +1 nucleosomal positions were extracted as the first nucleosomal position after TAIR10 annotated transcription start sites with a minimal overlap of 140 bp. The following nucleosomal positions were extracted following the definition of the +1 nucleosome for each gene.

Transcript profiling by RNA-seq

Nuclei were isolated from aerial parts of 6-DAS plants as previously described (51) and RNA was isolated using the TRIzol method (Invitrogen), before it was further purified and DNase-treated using the Monarch RNA Cleanup Kit (New England Biolabs) as previously described (42). Library preparation and RNAseq were carried out as described in the NuGEN Universal RNA-Seq with NuQuant User Guide v2.1 (Tecan Genomics), the Illumina NextSeq 500 System Guide (Illumina), and the KAPA Library Quantification Kit - Illumina/ABI Prism User Guide (Roche Sequencing Solutions). rRNA was depleted using the *A.thaliana* AnyDeplete module during the total RNA-Seq library preparation workflow (Tecan Genomics). This module contains probes targeting chloroplastic 4.5S, 16S and 23S rRNA as well as cytoplasmic 5.8S, 18S and 25S rRNA.

In brief, 25 ng of total RNA isolated from *Arabidopsis* nuclei were reverse transcribed into first strand cDNA using a mixture of random and poly-dT primers with an integrated DNase treatment step. Second strand synthesis, using a nucleotide analogue enabling strand retention, generated double stranded cDNA (ds cDNA). The ds cDNA was fragmented to a median size of 200–500 bp with a S2 Ultrasonication System (Covaris) using the following settings: intensity 5; duty cycle 10%; cycles per burst 200; treatment time 180 s; micro tube AFA fiber Snap-Cap. Next, end repair was performed to generate blunt-ended ds cDNA, followed by the ligation of the indexing adapters, a strand selection via nucleotide analogue-targeted degradation and a reduction of the *Arabidopsis* rRNA content by an AnyDeplete-mediated adaptor cleavage. Finally, cDNA libraries were created by 18 cycles PCR enrichment and purified by a magnetic bead clean-up using 0.8 volumes of the bead suspension. The libraries were quantified using the KAPA Library Quantification Kit. Equimolar amounts of each library were sequenced on a NextSeq 500 instrument controlled by the NextSeq Control Software (NCS) v2.2.0 using one 75 Cycles High Output Kit with the single index, single-read (SR) run parameters. Image analysis and base calling resulted in .bcl files, which were converted into .fastq files with the bcl2fastq v2.18 software.

Library preparation and RNAseq were performed at the Genomics Core Facility 'KFB—Center of Excellence for Fluorescent Bioanalytics' (University of Regensburg, Regensburg, Germany; www.kfb-regensburg.de). Sequencing of three biological replicates per genotype and condition resulted in an average of 8.4M reads per library (min 6.9M, max 14.4M) with an average Phred score > 34 (Table S2).

RNA-seq data analysis

Quality control of raw RNAseq reads was performed with FastQC v0.11.8 (https://www.bioinformatics.babraham.ac.uk/projects/fastqc/) and MultiQC (52). After the initial quality assessment, reads with low base quality and adapter contaminations were removed using Trimmomatic (v0.39) (45). The remaining reads were aligned to the TAIR10 genome assembly with STAR (v2.7.3a) (53). The resulting alignment maps were converted to .bam files with Samtools (v1.9) (47). Quality control of the alignment was performed with FastQC, MultiQC and Qualimap v2.2.1 (54). Read normalisation was performed with Samtools and Deeptools v3.3.0 (48). Count table was made with subread package v1.6.3 (55). Consistency of the biological replicates was evaluated by calculation of pairwise correlations and principle component analyses (Supplementary Figure S3, S4). Differential expression analysis was performed with DeSeq2 v1.24.0 (56). Unnormalised .bam alignment files were merged and then indexed with Samtools v1.9. $\log_2$ ratios of the HS libraries were calculated using the merged no HS control for each genotype as control with parallel sequencing depth normalisation with bamCompare (Deeptools v3.3.0). Internal exons and intron/exon borders were extracted using the R package TxDb.Athaliana.BioMart.plantsmart28 (version 3.2.2) with R (version 3.6.1).

Results

Differential distribution of TEFs over transcribed regions

Chromatin immunoprecipitation combined with high throughput sequencing (ChIP-seq) was used to map the distribution of TEFs and RNAPII genome-wide. To detect native SPT4–SPT5, PAF1C and FACT, antibodies directed against *Arabidopsis* SPT5-2, ELF7 (orthologue of PAF1) and SSRP1/SPT16 (22,25,34) were used. To detect elongating RNAPII, commercial antibodies were used that are directed

against the phosphorylated residues S2P and S5P of the heptapeptide repeats occurring in the CTD of the NRPB1 subunit (57). Analysis of the ChIP-seq data obtained with 14 days after stratification (DAS) Col-0 plants demonstrated that expectedly elongating RNAPII and TEFs are detected over RNAPII-transcribed regions (Figure 1A–C). RNAPII-S2P and S5P show a divergent pattern with the S2P signal gradually increasing from the transcriptional start site (TSS) towards the transcriptional end site (TES) and exhibiting a prominent peak just downstream of the TES, while S5P is more evenly distributed throughout the gene body. The distribution of RNAPII-S2P and S5P over transcribed regions (Supplementary Figure S5) is essentially in agreement with earlier studies in *Arabidopsis* (43,58). Moreover, as recently discussed (21), the result confirms the different genomic distribution of S5P in *Arabidopsis* in comparison to that observed in yeast and mammals, which exhibits maximum enrichment around the TSS with markedly declining coverage over the transcribed region towards the TES. The profile of SPT5 closely resembles that of S2P (Figure 1A), also evident from the high Pearson correlation of 0.95 (Supplementary Figure S6). ELF7 is spread over the transcribed region and no clear enrichment is seen at the TES (Figure 1B). The FACT subunits, SSRP1 and SPT16, share a highly similar distribution (Figure 1C) with a Pearson correlation of 0.99 (Supplementary Figure S6), which also illustrates the robustness of the analysis. The FACT occupancy over the transcribed region is shifted towards the TSS (relative to that of RNAPII) and more closely resembling the distribution of S5P rather than S2P. In line with their concerted involvement in transcriptional elongation the analysed TEFs and RNAPII-S2P/S5P share relatively high pairwise correlations (Supplementary Figure S6). Further analysis of the distribution patterns by hierarchical clustering confirmed the more pronounced conformity of SPT5 with S2P, and the higher conformity of FACT and ELF7 with S5P (Figure 1D). Next the analysed genes were divided into quartiles depending on the corresponding transcript levels (Supplementary Table S3). SPT5 shows a very clear linear correlation with S2P, while ELF7 shows a marked correlation with S5P and it is somewhat overrepresented in the gene body of very highly transcribed genes (Figure 2). Both SPT16 and SSRP1 exhibit striking similarity with each other and are (compared to S2P and S5P) overrepresented in the gene body of genes dependent of transcriptional activity (Figure 2). To identify regions of TEF enrichment relative to RNAPII, the ChIP-seq signals were analysed by differential peak calling of SPT5/ELF7/FACT relative to RNAPII-S2P/S5P. This analysis revealed that in line with the above results SPT5 largely shared the distribution of RNAPII-S2P, but (other than ELF7 and FACT) was enriched upstream of the TSS relative to RNAPII-S5P (Figure 3A). Consistently, relative to S5P, SPT5 is enriched mostly outside transcribed regions (Figure 3D, E). The enrichment of ELF7 is essentially restricted to the gene body (Figure 3B), where it co-localises with S5P rather than S2P (Figure 3D, E). For FACT a characteristic accumulation is detected downstream of the TSS (Figure 3C). This prominent promoter-proximal accumulation is seen both relative to S2P and S5P (Figure 3D, E). Analysis of the genes associated with the three TEFs revealed that 540, 907 and 1260 genes show peaks only for ELF7, SPT5 or SSRP1 and that a considerable portion of 1386 genes are enriched in both ELF7 and SSRP1 peaks (Supplementary Figure S7A). In line with that, the genes enriched in the different TEFs classify into essentially

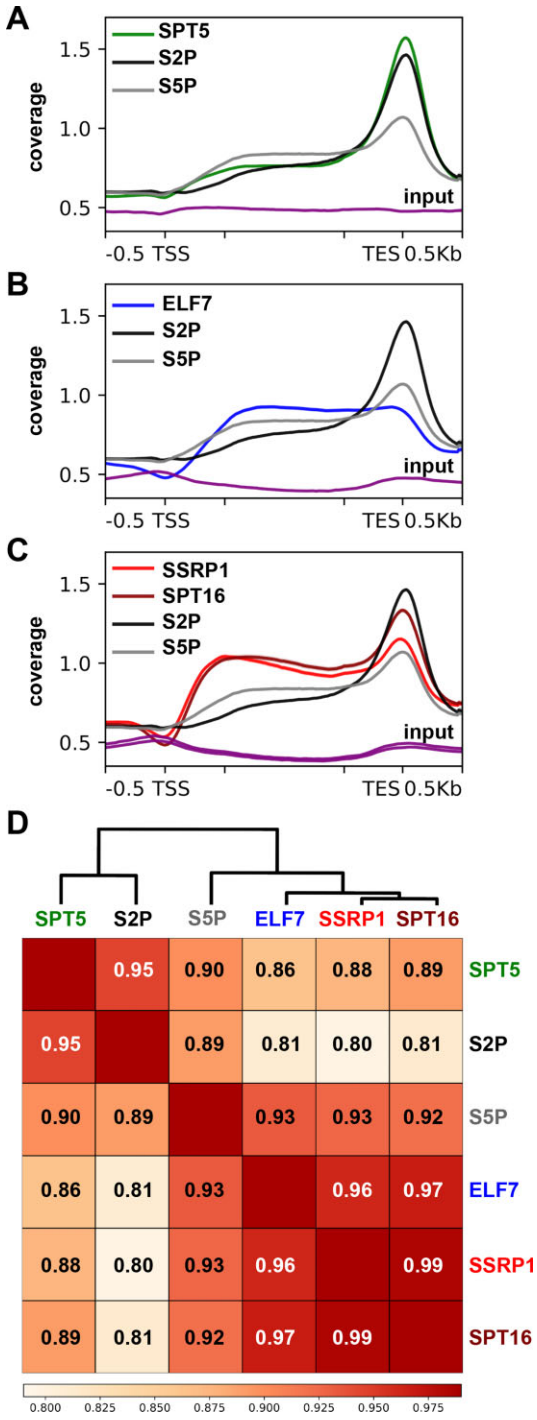

Figure 1. Elongation factors exhibit distinct distribution over transcribed regions relative to each other and relative to RNAPII. (**A–C**) Metagene profiles of TEFs and elongating RNAPII (S2P and S5P) distribution based on ChIP-seq data (based on four replicates for SPT5, ELF7, SSRP1, SPT16 and two replicates for S2P, S5P). TEF and RNAPII ChIP-seq coverage (normalised to counts per million reads) was plotted over TAIR10 annotated, non-overlapping, protein coding genes ($n = 24\,474$). Lines are colour-coded as indicated and represent the accumulation of RNAPII and elongation factors, while the shaded area indicates the standard error of the mean. For comparison input samples of the respective TEF ChIPs are shown. Genes were scaled over the annotated region and 500 bp upstream and downstream of TSS and TES are shown unscaled. (**D**) Pearsson correlation together with hierarchical clustering illustrates the differential distribution of TEFs and RNAPII. Pairwise correlation was calculated over all TAIR10 annotated, non-overlapping, protein coding genes ($n = 24\,474$) divided into 10 bins per gene.

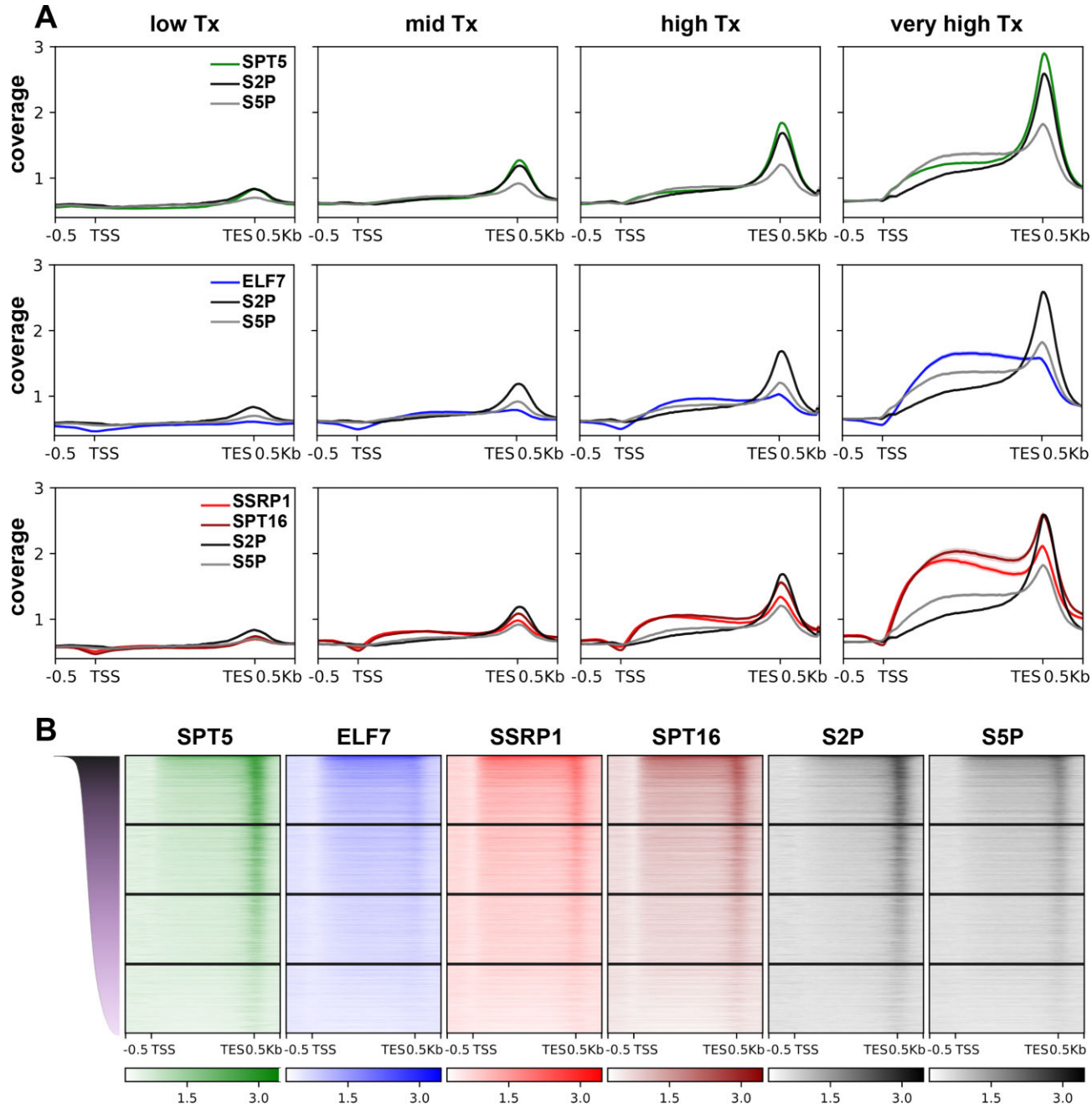

Figure 2. RNAPII and elongation factor occupancy increases with transcript levels. (**A**) Enrichment of elongating RNAPII (S2P, S5P) and elongation factors (SPT5, ELF7, SSRP1, SPT16) along transcribed regions depicted as metagene plots based on ChIP-seq data. Genes were divided into four groups according to transcript levels (logTPM, transcripts per million) based on RNA-seq data of Col-0 plants (n = 6177 in each group with quartile 'low Tx': logTPM 0.0 to -1.9; quartile 'mid Tx': logTPM 0.6 to 0.0; quartile 'high Tx': logTPM 0.9 to 0.6; quartile 'very high Tx': logTPM 3.4 to 0.9). Lines are colour-coded as indicated and represent the normalised coverage of RNAPII and elongation factors, while the shaded area indicates the standard error of the mean. (**B**) Differential occupancy of RNAPII and elongation factors along transcribed regions dependent on transcript levels shown as heatmaps. Genes are divided in four groups depending on transcript levels (as in (A); $n = 6177$) and they are sorted from high expression (top) to low expression (bottom) as indicated on the left as color-coded logTPMs (transcripts per million) of genes in Col-0 (no HS).

different GO terms (Supplementary Figure S7B). To assess the influence of the three TEFs on the distribution of elongating RNAPII, the genome-wide occupancy of RNAPII-S2P was analysed by ChIP-seq in plants deficient in the three TEFs relative to Col-0. SPT4-RNAi plants (termed *SPT4-R3*, also depleted in SPT5, (22)), *elf7-3 (*no full-length *ELF7* mRNA is detectable (26)), *ssrp1-2 (*substantially decreased expression of SSRP1 (37)) and for comparison Col-0 wildtype were comparatively analysed (Supplementary Figure S8). Over transcribed regions of genes corresponding to low or mid transcript levels hardly a difference in RNAPII-S2P occupancy is evident in the various genotypes under standard growth conditions. At genes with high or very high transcript levels compared to Col-0, in *elf7* and *ssrp1* plants a lower RNAPII-S2P coverage was detected. In *SPT4-R3* plants the RNAPII-S2P occupancy was rather increased, particularly in the region between TSS and TES. Taken together, these analyses illustrate that over transcribed *Arabidopsis* genes SPT4–SPT5, PAF1C and FACT are differently distributed relative to each other and relative to RNAPII.

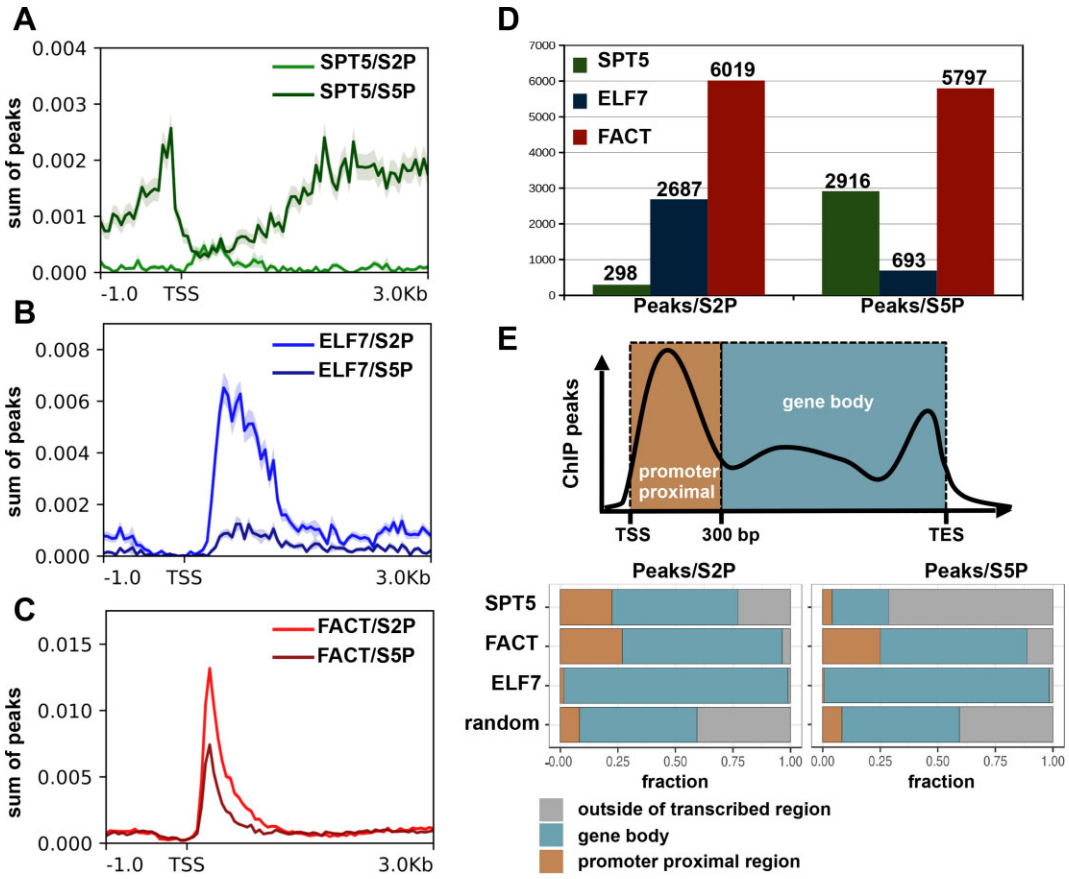

Figure 3. Genomic distribution of the TEFs relative to RNAPII-S2P and -S5P. (**A–C**) Metagene profiles of differential calling of ChIP-seq peaks obtained for SPT5, ELF7 and FACT (SSRP1, SPT16) relative to those obtained for RNAPII-S2P (TEF/S2P) and S5P (TEF/S5P). Lines are colour-coded as indicated and represent the accumulation of elongation factors relative to RNAPII, while the shaded area indicates the standard error of the mean. Please note the different scale of the y-axes. (**D**) Number of detected, differential peaks relative to S2P and S5P. (**E**) Genomic distribution of the detected differential peaks. Schematic diagram on top depicting the proximal region (0–300 bp downstream of TSS) and gene body (transcribed region without 0–300 bp). Bottom scheme depicts the distribution of the differential peaks relative to S2P and S5P in the promoter proximal region, gene body and outside of transcribed regions. For comparison, the distribution of randomly called peaks within the genome is shown (random).

Transcriptional reprogramming is distinctly affected in plants lacking different TEFs

To further elaborate the function of the TEFs in transcriptional elongation, *in vitro* grown plants deficient in TEFs (mentioned above) in comparison to Col-0 were subjected to heat stress (HS) to prompt transcriptional reprogramming. 6-DAS plants were exposed to a rapid HS of 10 min at 44°C (using a water bath to achieve fast temperature change), adapting an established protocol (41). Sublethal HS treatment of that kind evoked altered expression of hundreds of genes (42,59) and we presumed that this scenario may assist identifying whether/which transcriptional impairments occur in the different mutants. To examine genome-wide transcriptional changes of the plants deficient in TEFs relative to Col-0 upon exposure to heat, nuclear RNA was isolated from untreated plants (no HS) and plants exposed to HS. We intended to generate information on transcriptional output (freshly synthesised unspliced/spliced mRNAs including nascent transcripts) rather than steady-state mRNA levels obtained with total poly (A) mRNA enrichment (60,61). Therefore, we (i) isolated nuclear RNA (rather than total RNA), (ii) used rRNA depletion (rather than poly (A) enrichment) and (iii) made use of low RNA size cut-off (≥25 nt). Isolated RNAs were assayed by high throughput sequencing and the reads were mapped to the *Arabidopsis* genome. The log-fold change (LFC) in transcript coverage between the respective mutant and Col-0 is plotted without HS and after HS (Figure 4). The graphs indicate the mean LFC change over non-overlapping, protein coding genes. Under standard conditions relatively mild changes in the transcript patterns are observed for the mutants deficient in the three TEFs relative to Col-0 plants and the defects are increased with higher transcript levels (Figure 4A–C, top panels). Upon HS, however, pronounced and distinct defects are detected for the three genotypes. A common feature evident from the metagene profiles is a transcript level-dependent shift of the mapped RNA-seq reads towards the TSS (Figure 4A–C, bottom panels). In parallel, the transcript reads decrease along the transcribed region towards the TES, indicating decreased RNAPII processivity. This effect is most pronounced with *elf7*, while with *ssrp1* a prominent peak just downstream of the TSS becomes apparent upon HS. In case of *SPT4-R3* the drop in transcript reads over the transcribed region is less pronounced than with *elf7*. The relative shift of the RNA-seq reads towards the TSS and the decrease over the transcribed regions upon HS among the expressed gene groups is obvious over a large set of genes (Figure 4D–F). Thus, the transcript profiling analysis highlights that the depletion of TEFs distinctly impairs transcript synthesis at different genomic re-

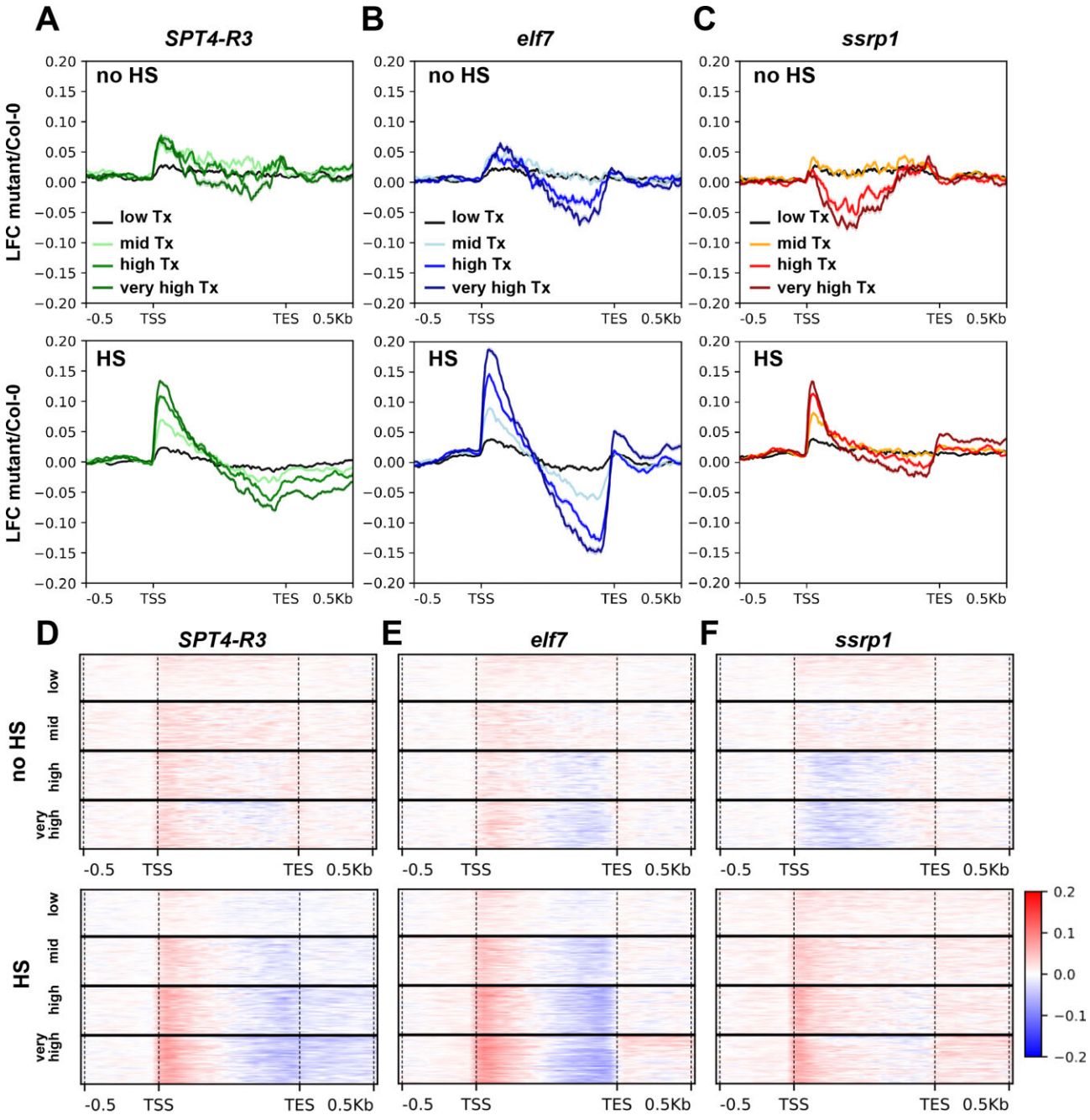

Figure 4. Mutants deficient in elongation factors exhibit distinct transcriptional defects. RNA-seq data (based on three replicates per genotype and condition) of mutants deficient in elongation factors (**A**, *SPT4-R3*; **B**, *elf7*; **C**, *ssrp1*) relative to Col-0 wildtype plants after 10 min HS (HS) or without HS (no HS). TSS-centred metagene profiles of the sequencing data split according to expression level of genes after HS into four groups as indicated (low Tx, mid Tx, high Tx and very high Tx with $n = 6177$ genes for each group). Replicates were merged and the log-fold changes (LFC) between mutant and Col-0 of no HS versus HS were calculated with TPM normalisation. (**D–F**) Heatmaps illustrate the shift of mapped RNA-seq reads of the transcribed gene groups ($n = 6177$) towards the TSS upon exposure to HS.

gions, particularly under conditions of massive transcriptional reprogramming.

In addition to transcribed regions SPT5 localises to a region upstream of TSSs

SPT5 mainly localises to the transcribed region, closely resembling the distribution of RNAPII-S2P (Figure 1). Differential ChIP-seq peak calling revealed that relative to S5P, SPT5 is also enriched upstream of the TSS (Figure 3). When summarising the differentially called ChIP-seq peaks over closely spaced genes (<500 bp distance) and more distant genes (>500 bp distance), it became clear that a notable SPT5 peak upstream of TSSs is detected only at closely spaced genes (Figure 5A). Unlike SPT5, independent from the gene distance, FACT and ELF7 exhibit no considerable enrichment in this region flanking the TSS (Supplementary Figure S9A–C). The SPT5 peak adjacent to transcribed regions reminded of the genomic distribution of BORDER proteins (BDR1-3) that were reported to prevent transcriptional interference of

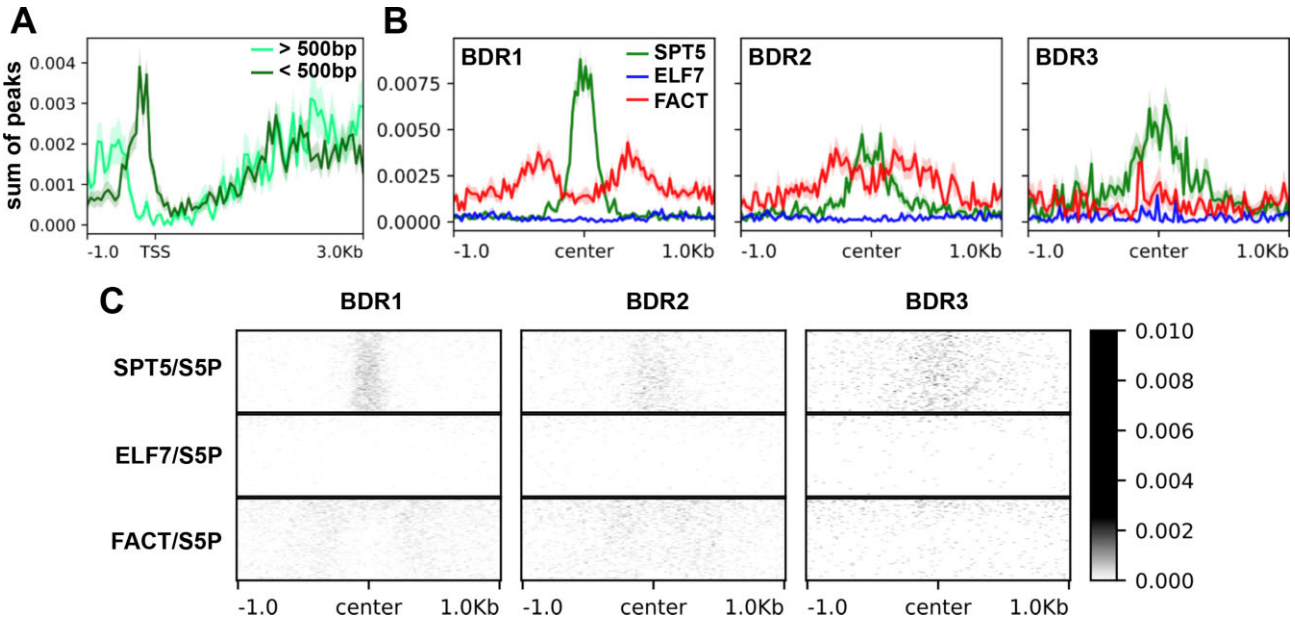

Figure 5. Beyond its prevalent coverage over transcribed regions, ChIP-seq peaks of SPT5 enriched relative to RNAPII-S5P are detected upstream of TSSs of closely spaced genes and correlate with BDR1 peaks. (**A**) TAIR10 annotated, non-overlapping, protein coding genes were divided into two classes according to their distance to the next annotated gene. Genes with less than 500bp distance to the TSS or TES of the next annotated gene were classified as closely spaced (<500 bp; $n = 9544$), while genes with more than 500 bp distance were classified as not closely spaced (>500 bp; $n = 7668$). SPT5 ChIP-seq peaks were centred to the TSS. (**B, C**) ChIP-seq peaks of SPT5, ELF7 and FACT were centred over ChIP-seq summits ($n = 21\,334$) of BDR1-3 (62). Lines (in A, B) are colour-coded as indicated and represent the accumulation of elongation factors, while the shaded area indicates the standard error of the mean.

closely spaced downstream genes in *Arabidopsis*. BDR1/2 occupied regions just upstream of the TSS and/or downstream of the TES, while BDR3 showed a strong preference for the TES (62). Reanalysis of the BDR1 ChIP-seq data demonstrated a more pronounced enrichment at closely spaced genes (<500 bp distance) when compared to more distant genes (>500 bp distance) (Supplementary Figure S9D). Peaks of SPT5 enrichment relative to RNAPII-S5P were centred over BDR1-3 ChIP-seq summits (62). This analysis demonstrated that SPT5 co-localises predominantly with BDR1 upstream of TSSs, whereas SSRP1 and ELF7 do not share this genomic distribution (Figure 5B). The heatmap shows a relative accumulation of SPT5 particularly over the centre of BDR1 peaks while ELF7 and FACT are not enriched (Figure 5C). The colocalization of SPT5 and BDR1 is also evident from genome browser views, illustrating individual genes (Supplementary Figure S10). Additionally, these views show that SPT5 is not enriched at all BDR1 peaks. Comparative analysis of SPT5 and BDR1 peaks observed at closely spaced (<500 bp distance) or more distant genes (>500 bp distance) illustrated a weak correlation between the presence of SPT5 and BDR1 and lesser distance of the analysed genes (Supplementary Figure S11). Therefore, unlike PAF1C and FACT, SPT5 associates with BDR1 target sites upstream of TSSs of closely spaced genes.

ELF7 is required for RNAPII to transcribe efficiently over splice sites

ELF7 was detected over transcribed regions and its distribution showed a lower correlation with RNAPII than that of SPT5 (Figure 1). Furthermore, ELF7 exhibits differences in the distribution compared to S2P but almost no difference to S5P (Figure 3B), and compared to Col-0 in *elf7* mutant plants, transcript reads decreased along transcribed regions, particularly upon HS-induced transcriptional reprogramming (Figure 4). In search of gene characteristics that may be related to ELF7-dependent transcriptional defects, genes up- and downregulated in *elf7* relative to Col-0 upon HS were analysed for the length of their transcribed regions. For downregulated genes a median length of 2532 bp was determined, whereas upregulated genes were shorter (median: 1787 bp) (Supplementary Figure S12A), suggesting that PAF1C is particularly required for transcription of longer genes. Moreover, downregulated genes contained ∼8.8 exons and upregulated genes contained fewer exons (∼6.2 exons), while exon length differed only slightly (160 versus 185 bp) between the two groups of genes (Supplementary Figure S12B, C). Genes downregulated in *elf7* show an increased transcript coverage throughout the gene body in Col-0, while this upregulation cannot be seen in *elf7* (Figure 6A). However, this difference between Col-0 and *elf7* is only apparent downstream of the promoter-proximal region. Therefore, genes downregulated in *elf7* are downregulated due to defective elongation beyond the promoter-proximal region (Figure 6A). For genes upregulated in *elf7* only minor differences are seen over the transcribed region (Figure 6B). This indicates a distinctive reduction of transcription along transcribed regions in ELF7-dependent genes. As genes downregulated in *elf7* contained a higher number of introns (Supplementary Figure S12C), RNA-seq data of intron-less genes were compared with those of intron-containing genes. Intron-less genes showed a similar pattern in *elf7* and Col-0, whereas for intron-containing genes transcript reads were reduced in *elf7* along the transcribed region (Figure 6C, D). To further analyse the possible correlation of transcriptional changes with the presence of introns, seen in *elf7* in comparison to *ssrp1* and *SPT4-R3*, LFCs of the respective mutant relative to Col-0 was plotted over annotated intron/exon borders of non-overlapping, protein-coding genes. Plotting the relative transcript coverage

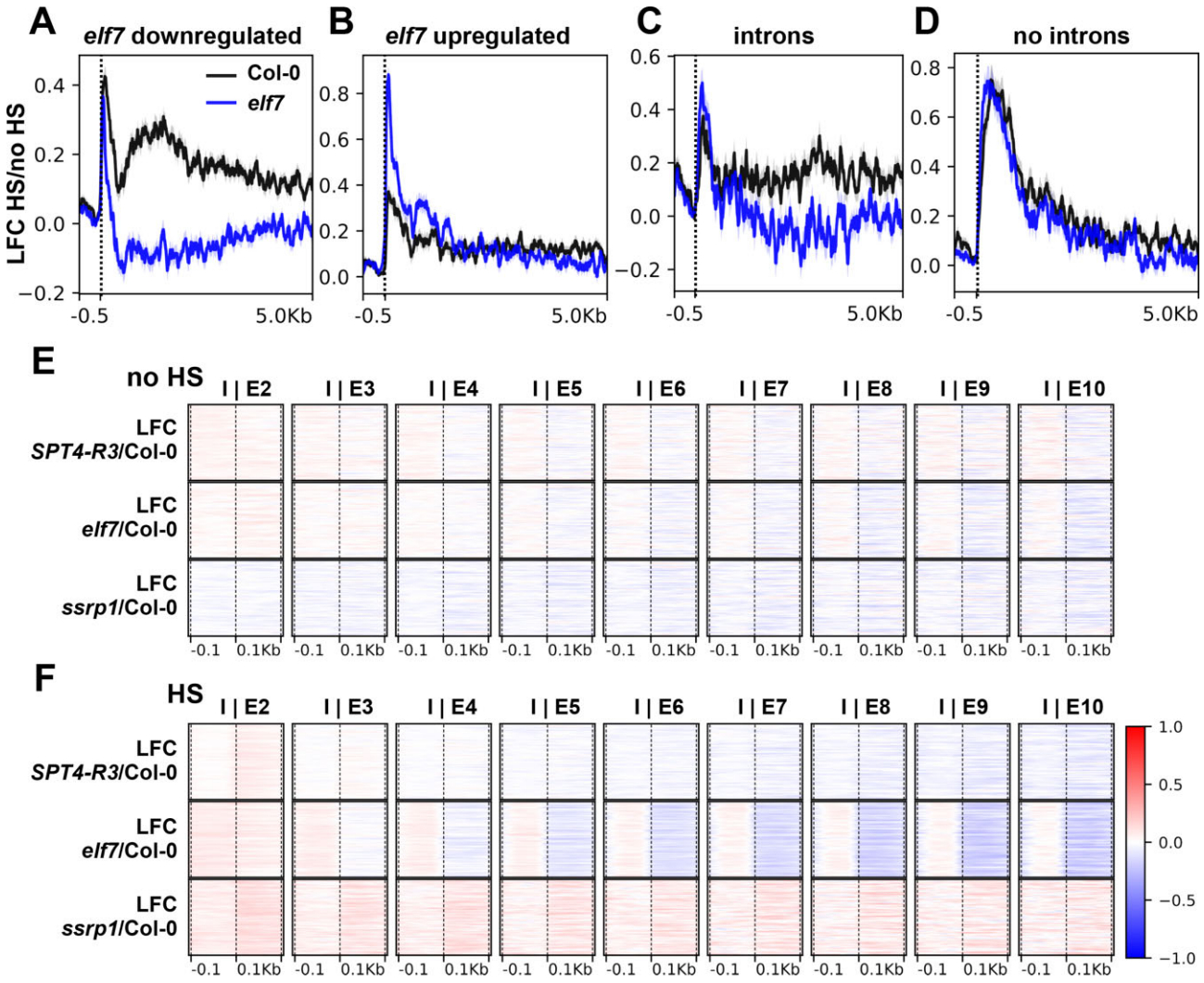

Figure 6. The transcription defects observed in *elf7* plants over transcribed regions are correlated with intron/exon borders. (**A**) RNA-seq data of HS relative to no HS (LFC) for *elf7* and Col-0 plants plotted over genes downregulated in *elf7* compared to Col-0 ($n = 290$), centred to the TSS (position of TSS is indicated by a dotted line). (**B**) RNA-seq data of *elf7* and Col-0 plants of HS relative to no HS (LFC) plotted over genes upregulated in *elf7* compared to Col-0 ($n = 129$), centred to the TSS. (**C**) RNA-seq data of *elf7* and Col-0 plants of HS relative to no HS (LFC) plotted over genes highly expressed upon HS containing ≥10 introns ($n = 290$), centred to the TSS. (**D**) RNA-seq data of *elf7* and Col-0 plants of HS relative to no HS (LFC) plotted over genes highly expressed upon HS containing no introns ($n = 355$), centred to the TSS. (E, F) RNA-seq data (LFC) of the respective mutant relative to Col-0 with no HS (**E**) and upon HS (**F**) over TAIR10 annotated intron/exon borders (I/E) of non-overlapping, protein-coding genes (n = 24474). From left to right consecutive intron/exon borders are depicted (starting on the left with I/E2 to I/E10 on the right). Dotted line indicates intron/exon borders.

over intron/exon borders along protein coding genes showed only minor differences under standard conditions (without HS) (Figure 6E). In *elf7* and *SPT4-R3* a slight reduction of mapped reads can be seen across intron/exon borders. However, upon HS a pronounced drop of transcripts is detected in *elf7* over intron/exon borders that is cumulative over successive intron/exon borders along genes (Figure 6F). These effects are clearly weaker for *SPT4-R3* and not discernible for *ssrp1* plants. Plotting the distribution of RNA-seq reads over ELF7 ChIP-seq peaks shows that this transcriptional defect is also present over ELF7 enriched regions (Supplementary Figure S12D, top). At the same time these ELF7 enriched sites exhibit accumulation of S5P (Supplementary Figure S12D, bottom). This suggests that ELF7 enriched regions in Col-0 coincide with sites of transcription defects in *elf7* plants upon HS. Genes downregulated in *elf7* were additionally searched for the occurrence of prominent sequence motifs. The two most strikingly identified motifs represent recognition sites for the spliceosomal factors SRSF2 and SNRNP (Supplementary Figure S12E), while no significantly enriched motifs were detected with genes upregulated in *elf7* or with the other analysed mutants (*ssrp1*, *SPT4-R3*). Analysis of the distribution of the two motifs demonstrated that the SRSF2 motifs map preferentially to intron/exon borders, while this is less prominent for the SNRNP motif (Supplementary Figure S12F). Hence, our analyses highlight that the transcriptional elongation defects observed with *elf7* plants correlate with the intron/exon structure of affected genes.

FACT localises to nucleosomes, correlates with the accessibility of NDRs and is required to promote transcription over +1 nucleosomes upon HS

The distribution of FACT over transcribed regions also showed a lower correlation with RNAPII than that of SPT5 (Figure 1) with a prominent promoter-proximal enrichment relative to RNAPII downstream of TSSs (Figure 3). Upon HS, transcript coverage accumulates in *ssrp1* plants just down-

stream of the annotated TSS (Figure 4). In view of the function of FACT as a histone chaperone, its genomic distribution was superimposed with nucleosome positions derived from MNase-seq data (42). This dataset was obtained by H3 immunoprecipitation after MNase digestion, ensuring that only DNA protected by histones is sequenced (63). Both the SSRP1 and SPT16 ChIP-seq coverage is enriched over nucleosomal positions, while the nucleosomal pattern is markedly less pronounced with ELF7 and SPT5 (Figure 7A) and RNAPII (Supplementary Figure S13A). Comparison of the FACT enrichment relative to RNAPII-S2P revealed that in general, the SSRP1 coverage correlates positively with the transcript level (Figure 7B). The accumulation of FACT at highly transcribed genes is in line with the analyses above (Figure 2). FACT (both SSRP1 and SPT16) and RNAPII are particularly enriched at genes that are downregulated in *ssrp1* plants relative to Col-0 upon HS, while the coverage is clearly lower at upregulated genes (Supplementary Figure S13B). With genes that are differentially expressed dependent on ELF7, the differences in ELF7 and RNAPII occupancy between up- and downregulated genes are comparatively clearly lower (Supplementary Figure S13C). This suggests that compared to PAF1C, FACT is particularly required for transcriptional upregulation in response to HS. Genes downregulated in *ssrp1* (relative to Col-0) in fact fail to be upregulated upon HS, while the genes differentially expressed in *elf7* show comparable S2P/S5P coverage in Col-0 (cf. Supplementary Figure S13B, C). Consistent with earlier studies (64,65), along transcribed regions of genes with high or medium expression, a notable, phased nucleosome pattern is evident that is not well discernible with low- or non-expressed genes (Figure 7B). Strikingly, high FACT occupancy is associated with a clearly more pronounced nucleosome-depleted region (NDR) upstream of the TSS. Using unsupervised k-means clustering, two gene clusters were identified according to high and low FACT occupancy relative to RNAPII-S2P based on the ChIP-seq data. Genes of both clusters were intersected with nucleosomal positions, and centring SSRP1/SPT16 ChIP-seq peaks to the +1 nucleosomal position of those genes demonstrated a distinctive accumulation of SSRP1 and SPT16 just downstream of the +1 nucleosome of FACT enriched genes (Figure 7C). Centring MNase histone H3 ChIP-seq data (42) over the +1 nucleosomal position of the FACT enriched gene cluster revealed a striking depletion of nucleosomes upstream of the TSS, while there is no marked change in the nucleosomal pattern downstream of the TSS (Figure 7D). The depletion of the NDR is considerably less pronounced with the FACT non-enriched gene cluster. The mean transcript levels of FACT enriched genes are higher than those of ELF7- and SPT5-enriched genes, suggesting that FACT is especially associated with high expression levels (Supplementary Figure S13D). In addition, the transcript levels of FACT non-enriched genes are lower, but still those genes are transcribed, although there is a relatively high nucleosome occupancy at the NDR. Centring the relative fold-change in transcript coverage (cf. Figure 4) over the two gene clusters highlighted a clear accumulation of transcripts just upstream of the +1 nucleosome in the FACT enriched gene cluster after HS (Figure 7E). The accumulation of transcript reads is distinctly weaker for the FACT non-enriched gene cluster or without HS treatment. The maximum accumulation of transcripts maps ∼40 bp upstream of the centre of the +1 nucleosome, while the peak centre of FACT enrichment maps ∼110 bp downstream of the +1 nucleosome (Figure 7F–H). Centring the FACT ChIP-seq coverage and the RNA-seq reads to the +1 to +5 nucleosomal positions illustrates that the distinctive FACT occupancy as well as the accumulating RNA-seq reads upon HS occur exclusively at the +1 nucleosome (Supplementary Figure S14A, B). Furthermore, we plotted FACT ChIP-seq peaks centred to the +1 nucleosome over FACT enriched/non-enriched, ELF7 enriched/non-enriched and SPT5 enriched/non-enriched gene clusters. The specific enrichment of FACT downstream of the +1 nucleosome is only detected in the FACT enriched cluster, but not in the other gene clusters (Supplementary Figure S15A-C). The corresponding MNase H3 ChIP-seq patterns reveal that the distinctive cleared NDR upstream of the TSS is obvious in the FACT enriched cluster, but clearly less marked in the other gene clusters (Supplementary Figure S15D-G). Finally, by plotting the MNase H3 ChIP-seq signal centred to the +1 nucleosome of genes up- or downregulated in *ssrp1*, the cleared NDR is quite evident for the downregulated genes, but markedly less discernible for the upregulated genes (Supplementary Figure S15H). Thus, the genes that exhibit particularly increased FACT coverage (Supplementary Figure S13B) are characterised by a prominent NDR upstream of the TSS (Supplementary Figure S15H) and require FACT for transcriptional upregulation. Apart from its influence on the promoter-proximal NDR our results imply that FACT is required under HS conditions for RNAPII to efficiently transcribe through +1 nucleosomes of a number of genes. Recently, the elongation factor TFIIS was found to be critically involved in plant HS response, in part also by promoting transcription through the +1 nucleosome (42,59). Therefore, we examined whether the expression of a common set of genes is affected in *tfIIs* and *ssrp1* upon HS. However, comparison of the genes downregulated upon HS revealed only a minor overlap between the genes affected in *tfIIs* and *ssrp1* (Supplementary Figure S16A). TFIIS-dependent stalling of RNAPII at the +1 nucleosome under HS conditions is associated with eviction of the histone variant H2A.Z from the +1 nucleosome (42). Hence, we examined H2A.Z occupancy in absence/presence of HS, derived from H2A.Z ChIP-seq data (66) over genes that were up- or downregulated in *ssrp1* relative to Col-0. No change in H2A.Z coverage at the +1 nucleosome was apparent in the analysis (Supplementary Figure S16B). Consequently, both FACT and TFIIS influence RNAPII transcription at the +1 nucleosome upon HS, but in different ways.

Discussion

Eukaryotic organisms vary substantially regarding genomic features that most likely influence the process of transcript elongation by RNAPII. Besides distinctions in chromatin characteristics this includes genome size and in part related to that enormous differences in the common length of transcribed regions, on the one hand in mammals (e.g. ∼66.6 kb in human, (67)) and on the other hand in *Arabidopsis* or yeast (e.g. ∼2.2 kb in *Arabidopsis*, (68)). Still, the majority of TEFs are conserved among eukaryotes indicating that they may be adapted to the respective genomic context and consequently to the specific requirements for efficient transcription. Here we have examined the genomic distribution of three different types of TEFs in *Arabidopsis* and investigated their role in transcriptional reprogramming by analysing the respective mutant plants under stress conditions.

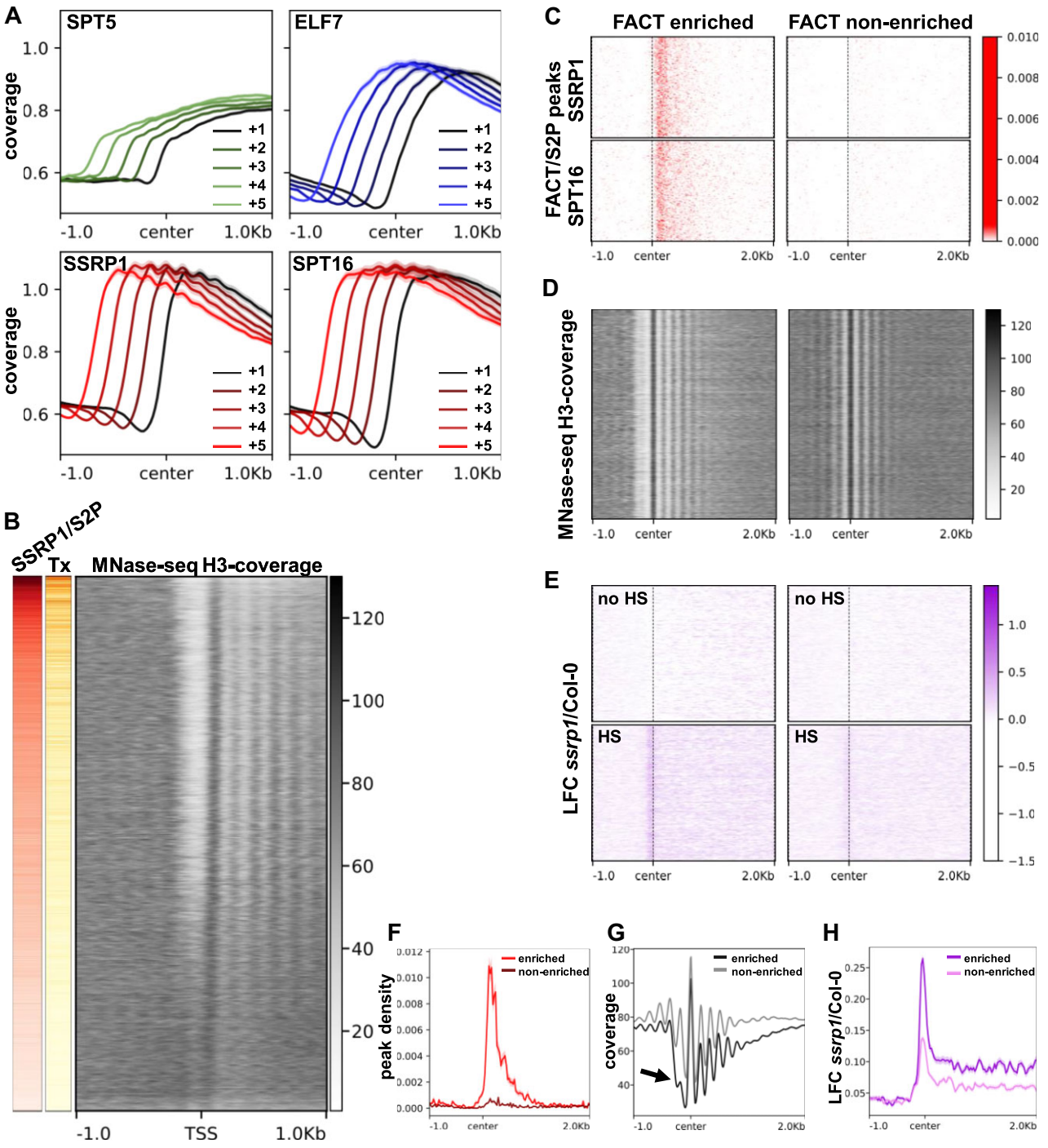

Figure 7. FACT is enriched over nucleosomal positions, correlates with the accessibility of the promoter-proximal NDR and upon HS is required for efficient transcription through +1 nucleosomes. (**A**) SSRP1 and SPT16 exhibit a more pronounced nucleosomal pattern than ELF7 and SPT5. The respective TEF ChIP-seq coverage was centred over nucleosome positions (+1 to + 5) from MNase H3 ChIP-seq data (n = 26295 for +1 nucleosome) (42). (**B**) Transcriptional activity (Tx, orange), SSRP1 relative to RNAPII-S2P enrichment (red) and mononucleosomal coverage (grey) over all TAIR10 annotated, non-overlapping, protein-coding genes sorted by mean SSRP1 signal intensity ($n = 24\,474$). (C–H) Peaks called from FACT (SSRP1 and SPT16) relative to RNAPII-S2P ChIP-seq data were divided into two clusters according to high FACT occupancy (FACT enriched; $n = 10\,360$) and low FACT occupancy (FACT non-enriched; $n = 13\,901$) using unsupervised *k*-means clustering. (**C**) Genes from both clusters were intersected with +1 nucleosomal positions. Called peaks from SSRP1 and SPT16 ChIP-seq data were centred to the +1 nucleosomal position in the respective cluster. (**D**) MNase H3 ChIP-seq data was centered to the +1 nucleosomal position in the respective cluster. (**E**) Based on the RNA-seq data, LFC of *ssrp1*/Col-0 without HS and after HS was centred over the +1 nucleosomal position in the respective cluster. (**F**) Mean density of FACT/S2P ChIP-seq peaks, (**G**) mean MNase H3 ChIP-seq coverage (NDR seen with the FACT enriched cluster indicated by an arrow) and (**H**) LFC of *ssrp1*/Col-0 based on RNA-seq after HS centered to the +1 nucleosomal position in the two above-mentioned gene clusters.

Our ChIP-seq analysis revealed that SPT5 associates with transcribed regions and its occupancy correlates with that of RNAPII, closely resembling the distribution of S2P. The enrichment of SPT5 at the TES (along with S2P) suggests that it remains associated with RNAPII until termination. Moreover, the SPT5 profile resembles that of the elongation factor ELF1 in *Arabidopsis* (69), which is in line with the synergistic action of yeast SPT4–SPT5 and ELF1 on *in vitro* transcript elongation on nucleosomal templates (70). In mammals, there is a prominent promoter-proximal SPT5 peak close to the TSS at the same position as that of another TEF termed NELF (71), consistent with the role of SPT4–SPT5 and NELF in establishment/release of RNAPII promoter-proximal pausing immediately down-stream of TSSs (13,14). Yeast and plants do not encode NELF and supposedly do not make use of stable, regulated promoter-proximal pausing of RNAPII the way mammals do (21,72) and in agreement with that no promoter-proximal SPT5 peak is observed in yeast (73,74) and *Arabidopsis* (Figures 1 and 2). In mammals and yeast, SPT4–SPT5 stabilises the elongation complex and increases RNAPII processivity and elongation rate (75–78) consistent with its strategic position on the elongating polymerase (79). In accord with a reduced elongation rate (80), an increased coverage of RNAPII-S2P occurred at highly transcribed genes in *SPT4-R3* plants under normal conditions, as previously observed (22). Upon exposure to HS, decreased mapping of transcript reads was detected along the transcribed region towards TES in *SPT4-R3* plants, indicative of reduced RNAPII processivity. Apart from its predominant association with transcribed regions, a peak of SPT5 was detected upstream of TSSs of some closely spaced genes. There it co-localises with BDR1 that has been reported to prevent transcriptional interference with closely spaced downstream genes (62). While the SPT5 peaks co-localise with BDR1 summits, it is uncertain whether the accumulation close to TSSs might be an interference with peaks at TESs of neighbouring genes. The functional implication of SPT5 localising upstream of TSSs is unclear, but it may be related to a possible involvement in transcriptional initiation as proposed for mammalian SPT5 (81).

The *Arabidopsis* PAF1C subunit ELF7 is almost exclusively distributed over the transcribed region of protein-coding genes and shows a higher correlation with S5P rather than S2P. Thus, the genomic distribution largely resembles that of the yeast orthologues, which are detected along the gene body with declining occupancy at the TES (73,74). In mammals, PAF1C exhibits a notably different distribution, as in addition to its occupancy over the transcribed region, remarkable enrichment of PAF1C is detected at TSSs and downstream of TESs (82). We noticed in *elf7* plants a striking decline of transcript reads along the transcribed region towards TES after exposure to HS that was more pronounced with longer genes, suggesting reduced processivity. PAF1C has the capacity to stabilise the elongation complex, which facilitates transcript elongation on chromatin templates resulting in enhanced processivity (83–86). Our analyses of the transcriptional defects observed in *elf7* plants revealed a link with the occurrence of introns. Metagene profiles over genes with introns show decreased transcript coverage in *elf7* downstream of the promoter-proximal region and the effect was cumulative over consecutive intron/exon borders. The sites of impaired transcript mapping are also characterised by elevated ELF7 occupancy and are enriched in RNAPII-S5P, which is linked to co-transcriptional splicing (87,88). Ongoing transcription and co-transcriptional intron splicing are closely coupled, which is manifested by physical interactions between the RNAPII elongation complex and the splicing machinery that has been also demonstrated in *Arabidopsis* (25). In various organisms including plants, transcriptional elongation and splicing were found to influence each other in complex and not completely clarified manners (87–90). In this scenario, PAF1C could facilitate recruitment of splicing factors such as NTC, facilitating intron splicing (91,92) and/or SRSF2/SNRNP, whose recognition motifs were markedly enriched in genes downregulated in *elf7*. As a consequence of splicing defects transcriptional elongation may be indirectly impaired. Just as well the above-mentioned stabilisation of the elongation complex by PAF1C (83–86) could promote RNAPII transcription across intron/exon borders, resulting in enhanced processivity. In view of functional differences that were observed between PAF1C subunits (15,21), it remains to be seen, whether our findings related to ELF7 are representative of the entire PAF1C complex.

The FACT subunits, SSRP1 and SPT16, co-localise over transcribed regions and compared to RNAPII-S2P/S5P are shifted towards the TSS particularly at highly transcribed genes. The distribution of *Arabidopsis* FACT is similar to that observed in yeast, while in metazoa FACT is even more enriched downstream of the TSS, which may be related to the regulated RNAPII promoter-proximal pausing (73,93). Beyond that FACT displayed a nucleosomal periodicity over transcribed genes, corresponding to that of yeast FACT. There, the periodicity was interpreted as preferential binding of FACT to nucleosomes partially unwrapped by transcribing RNAPII (94–96). This is in agreement with recent structural studies, demonstrating that upon unwrapping DNA from the TSS-proximal side of the nucleosome by the approaching RNAPII elongation complex and exposure of the proximal H2A-H2B dimer, FACT is recruited to assist further nucleosome transcription (97,98). Upon HS in *ssrp1* plants (in which SSRP1 is downregulated to <50%, (37)) transcript reads accumulated just upstream of the +1 nucleosome, close to the site of FACT enrichment (Figure 7). This suggests that under HS conditions FACT is required for early transcript elongation, particularly for efficient transcription through the +1 nucleosome. Since there is only minor overlap between differentially expressed genes in *tfIIs* (42) and *ssrp1* relative to Col-0 upon exposure to HS, it is likely that TFIIS and FACT distinctly affect transcription through the +1 nucleosomes. Consistently, the maximum accumulation of transcripts upon HS map ∼40 and ∼20 bp upstream of the +1 nucleosome centre in *ssrp1* and *tfIIs*, respectively. Similar to yeast FACT (96), *Arabidopsis* FACT accumulates downstream of the +1 nucleosome. Early transcript elongation appears to be remarkably responsive to altered temperatures in *Arabidopsis*, as promoter-proximal accumulation of RNAPII downstream of TSS occurs both upon exposure to cold and heat (42,99,100). Another striking feature related to FACT was the occurrence of a prominent NDR upstream of the TSS at FACT enriched genes that is not seen with FACT non-enriched genes or with genes enriched in ELF7 or SPT5. Depletion of FACT from mouse cells leads to a loss of promoter-proximal nucleosomal occupancy resulting in a NDR upstream of TSSs that is associated with increased transcription (101). As in our experimental setup, the MNase cleavage was followed by H3-ChIP before sequencing, we conclude that the highly MNase sensitive region upstream of TSSs of FACT enriched genes is de-

pleted in nucleosomes. This is consistent with earlier experiments that revealed that at a subset of genes phosphorylation of *Arabidopsis* SPT16 is required to establish or retain a NDR upstream of the TSS (44). NDRs play important roles in regulating RNAPII transcription as they are sites of transcription factor binding, preinitiation complex assembly and RNAPII loading (102,103). Thus, in *Arabidopsis* and mouse the histone chaperone FACT modulates nucleosome occupancy upstream of TSSs and in *Arabidopsis* FACT is particularly required upon HS for the efficient upregulation of genes. The applied rapid HS results in a massive transcriptional reprogramming of hundreds of genes (42,59), hence apparently necessitating FACT activity to adapt to the altered conditions.

Our study analysing the genomic occupancy of three types of RNAPII elongation factors in plants revealed that SPT4–SPT5, PAF1C and FACT predominantly localise to transcribed regions, albeit with distinct distribution patterns. Examination of corresponding mutant plants under acute HS conditions highlighted that different TEFs are diversely required to elicit an appropriate transcriptional response. These insights into post-initiation regulation of gene activity in *Arabidopsis* will serve as a foundation for future studies addressing transcript elongation also in other plant species. Moreover, it represents a starting point for comparative studies to unveil the similarities and dissimilarities of RNAPII transcriptional regulation relative to yeast and metazoan models.

Data availability

ChIP-Seq data and RNA-Seq data was deposited at the sequence read archive under the BioProject PRJNA931822, PRJNA1006389 and PRJNA756828. Additional ChIP-Seq data was deposited in the Gene Expression Omnibus under the accession GSE241143. MNase-Seq and NET-Seq data is available under the BioProject PRJNA877815 and the GEO accession GSE117014, respectively.

Supplementary data

Supplementary Data are available at NAR Online.

Acknowledgements

We would like to thank Christoph Moehle und Thomas Stempfl for continuous support of this project regarding NGS.

Funding

German Research Foundation (DFG) [Gr1159/16-1, SFB960/A6 to K.D.G.]. Funding for open access charge: DFG.

Conflict of interest statement

None declared.

References

1. Svejstrup,J.Q. (2004) The RNA polymerase II transcription cycle: cycling through chromatin. *Biochim. Biophys. Acta*, **1677**, 64–73.
2. Sims,R.J., Belotserkovskaya,R. and Reinberg,D. (2004) Elongation by RNA polymerase II: the short and long of it. *Genes Dev.*, **18**, 2437–2468.
3. Jeronimo,C., Collin,P. and Robert,F. (2016) The RNA polymerase II CTD: the increasing complexity of a low-complexity protein domain. *J. Mol. Biol.*, **428**, 2607–2622.
4. Harlen,K.M. and Churchman,L.S. (2017) The code and beyond: transcription regulation by the RNA polymerase II carboxy-terminal domain. *Nat. Rev. Mol. Cell Biol.*, **18**, 263–273.
5. Mayer,A., Landry,H.M. and Churchman,L.S. (2017) Pause & go: from the discovery of RNA polymerase pausing to its functional implications. *Curr. Opin. Cell Biol.*, **46**, 72–80.
6. Noe Gonzalez,M., Blears,D. and Svejstrup,J.Q. (2021) Causes and consequences of RNA polymerase II stalling during transcript elongation. *Nat. Rev. Mol. Cell Biol.*, **22**, 3–21.
7. Chen,F.X., Smith,E.R. and Shilatifard,A. (2018) Born to run: control of transcription elongation by RNA polymerase II. *Nat. Rev. Mol. Cell Biol.*, **19**, 464–478.
8. Kwak,H. and Lis,J.T. (2013) Control of transcriptional elongation. *Ann. Rev. Genet.*, **47**, 483–508.
9. Osman,S. and Cramer,P. (2020) Structural Biology of RNA Polymerase II Transcription: 20 Years On. *Ann. Rev. Cell Dev. Biol.*, **36**, 1–34.
10. Ehara,H. and Sekine,S.-I. (2018) Architecture of the RNA polymerase II elongation complex: new insights into Spt4/5 and Elf1. *Transcription*, **9**, 286–291.
11. Schier,A.C. and Taatjes,D.J. (2020) Structure and mechanism of the RNA polymerase II transcription machinery. *Genes Dev.*, **34**, 465–488.
12. Hartzog,G.A. and Fu,J. (2013) The Spt4-Spt5 complex: a multi-faceted regulator of transcription elongation. *Biochim. Biophys. Acta*, **1829**, 105–115.
13. Decker,T.-M. (2021) Mechanisms of Transcription Elongation Factor DSIF (Spt4-Spt5). *J. Mol. Biol.*, **433**, 166657.
14. Song,A. and Chen,F.X. (2022) The pleiotropic roles of SPT5 in transcription. *Transcription*, **13**, 53–69.
15. Francette,A.M., Tripplehorn,S.A. and Arndt,K.M. (2021) The Paf1 complex: a keystone of nuclear regulation operating at the interface of transcription and chromatin. *J. Mol. Biol.*, **433**, 166979.
16. Jaehning,J.A. (2010) The Paf1 complex: platform or player in RNA polymerase II transcription?, *Biochim. Biophys. Acta*, **1799**, 279–388.
17. Formosa,T. and Winston,F. (2020) The role of FACT in managing chromatin: disruption, assembly, or repair?, *Nucleic Acids Res.*, **48**, 11929–11941.
18. Gurova,K., Chang,H.-W., Valieva,M.E., Sandlesh,P. and Studitsky,V.M. (2018) Structure and function of the histone chaperone FACT - resolving FACTual issues. *Biochim. Biophys. Acta*, **1861**, 892–904.
19. Jeronimo,C. and Robert,F. (2022) The histone chaperone FACT: a guardian of chromatin structure integrity. *Transcription*, **13**, 16–38.
20. van Lijsebettens,M. and Grasser,K.D. (2014) Transcript elongation factors: shaping transcriptomes after transcript initiation. *Trends Plant Sci.*, **19**, 717–726.
21. Obermeyer,S., Kapoor,H., Markusch,H. and Grasser,K.D. (2023) Transcript elongation by RNA polymerase II in plants: factors, regulation and impact on gene expression. *Plant J.*
22. Dürr,J., Lolas,I.B., Sørensen,B.B., Schubert,V., Houben,A., Melzer,M., Deutzmann,R., Grasser,M. and Grasser,K.D. (2014) The transcript elongation factor SPT4/SPT5 is involved in auxin-related gene expression in Arabidopsis. *Nucleic Acids Res.*, **42**, 4332–4347.
23. Xue,M., Zhang,H., Zhao,F., Zhao,T., Li,H. and Jiang,D. (2021) The INO80 chromatin remodeling complex promotes thermomorphogenesis by connecting H2A.Z eviction and active transcription in Arabidopsis. *Mol. Plant*, **14**, 1799–1813.
24. Liaqat,A., Alfatih,A., Jan,S.U., Sun,L., Zhao,P. and Xiang,C. (2023) Transcription elongation factor AtSPT4-2 positively modulates salt tolerance in Arabidopsis thaliana. *BMC Plant Biol.*, **23**, 49.

25. Antosz,W., Pfab,A., Ehrnsberger,H.F., Holzinger,P., Köllen,K., Mortensen,S.A., Bruckmann,A., Schubert,T., Längst,G., Griesenbeck,J., *et al.* (2017) The Composition of the Arabidopsis RNA Polymerase II Transcript Elongation Complex Reveals the Interplay between Elongation and mRNA Processing Factors. *Plant Cell*, **29**, 854–870.
26. He,Y., Doyle,M.R. and Amasino,R.M. (2004) PAF1-complex-mediated histone methylation of *FLOWERING LOCUS C* chromatin is required for the vernalization-responsive, winter-annual habit in *Arabidopsis*. *Genes Dev.*, **18**, 2774–2784.
27. Oh,S., Zhang,H., Ludwig,P. and van Nocker,S. (2004) A mechanism related to the yeast transcriptional regulator Paf1c is required for expression of the *Arabidopsis FLC/MAF* MADS box gene family. *Plant Cell*, **16**, 2940–2953.
28. Park,S., Oh,S., Ek-Ramos,J. and van Nocker,S. (2010) PLANT HOMOLOGOUS TO PARAFIBROMIN is a component of the PAF1 complex and assists in regulating expression of genes within H3K27ME3-enriched chromatin. *Plant Physiol.*, **153**, 821–831.
29. Yu,X. and Michaels,S.D. (2010) The *Arabidopsis* Paf1c complex component CDC73 participates in the modification of FLOWERING LOCUS C chromatin. *Plant Physiol.*, **153**, 1074–1084.
30. Nasim,Z., Susila,H., Jin,S., Youn,G. and Ahn,J.H. (2022) Polymerase II-associated factor 1 complex-regulated FLOWERING LOCUS C-clade genes repress flowering in response to chilling. *Front. Plant Sci.*, **13**, 817356.
31. Jensen,G.S., Fal,K., Hamant,O. and Haswell,E.S. (2017) The RNA polymerase-associated factor 1 complex is required for plant touch responses. *J. Exp. Bot.*, **68**, 499–511.
32. Obermeyer,S., Stöckl,R., Schnekenburger,T., Moehle,C., Schwartz,U. and Grasser,K.D. (2022) Distinct role of subunits of the Arabidopsis RNA polymerase II elongation factor PAF1C in transcriptional reprogramming. *Front. Plant Sci.*, **13**, 974625.
33. Zhang,H., Li,X., Song,R., Zhan,Z., Zhao,F., Li,Z. and Jiang,D. (2022) Cap-binding complex assists RNA polymerase II transcription in plant salt stress response. *Plant Cell Environ.*, **45**, 2780–2793.
34. Duroux,M., Houben,A., Růzicka,K., Friml,J. and Grasser,K.D. (2004) The chromatin remodelling complex FACT associates with actively transcribed regions of the Arabidopsis genome. *Plant J.*, **40**, 660–671.
35. Perales,M. and Más,P. (2007) A functional link between rhythmic changes in chromatin structure and the Arabidopsis biological clock. *Plant Cell*, **19**, 2111–2123.
36. Frost,J.M., Kim,M.Y., Park,G.T., Hsieh,P.-H., Nakamura,M., Lin,S.J.H., Yoo,H., Choi,J., Ikeda,Y., Kinoshita,T., *et al.* (2018) FACT complex is required for DNA demethylation at heterochromatin during reproduction in Arabidopsis. *Proc. Natl. Acad. Sci. U.S.A.*, **115**, E4720–E4729.
37. Lolas,I.B., Himanen,K., Grønlund,J.T., Lynggaard,C., Houben,A., Melzer,M., van Lijsebettens,M. and Grasser,K.D. (2010) The transcript elongation factor FACT affects Arabidopsis vegetative and reproductive development and genetically interacts with HUB1/2. *Plant J.*, **61**, 686–697.
38. Ma,Y., Gil,S., Grasser,K.D. and Mas,P. (2018) Targeted recruitment of the basal transcriptional machinery by LNK clock components controls the circadian rhythms of nascent RNAs in Arabidopsis. *Plant Cell*, **30**, 907–924.
39. Nielsen,M., Ard,R., Leng,X., Ivanov,M., Kindgren,P., Pelechano,V. and Marquardt,S. (2019) Transcription-driven chromatin repression of Intragenic transcription start sites. *PLoS Genet.*, **15**, e1007969.
40. Murashige,T. and Skoog,F. (1962) A revised medium for rapid growth and bioassay with tobacco tissue cultures. *Physiol.Plant*, **15**, 473–497.
41. Stief,A., Altmann,S., Hoffmann,K., Pant,B.D., Scheible,W.-R. and Bäurle,I. (2014) Arabidopsis miR156 regulates tolerance to recurring environmental stress through SPL transcription factors. *Plant Cell*, **26**, 1792–1807.
42. Obermeyer,S., Stöckl,R., Schnekenburger,T., Kapoor,H., Stempfl,T., Schwartz,U. and Grasser,K.D. (2023) TFIIS is crucial during early transcript elongation for transcriptional reprogramming in response to heat stress. *J. Mol. Biol.*, **435**, 167917.
43. Antosz,W., Deforges,J., Begcy,K., Bruckmann,A., Poirier,Y., Dresselhaus,T. and Grasser,K.D. (2020) Critical role of transcript cleavage in Arabidopsis RNA polymerase II transcriptional elongation. *Plant Cell*, **32**, 1449–1463.
44. Michl-Holzinger,P., Obermeyer,S., Markusch,H., Pfab,A., Ettner,A., Bruckmann,A., Babl,S., Längst,G., Schwartz,U., Tvardovskiy,A., *et al.* (2022) Phosphorylation of the FACT histone chaperone subunit SPT16 affects chromatin at RNA polymerase II transcriptional start sites in *Arabidopsis*. *Nucleic Acids Res.*, **50**, 5014–5028.
45. Bolger,A.M., Lohse,M. and Usadel,B. (2014) Trimmomatic:a flexible trimmer for Illumina sequence data. *Bioinformatics*, **30**, 2114–2120.
46. Langmead,B. and Salzberg,S.L. (2012) Fast gapped-read alignment with Bowtie 2. *Nat. Meth.*, **9**, 357–359.
47. Danecek,P., Bonfield,J.K., Liddle,J., Marshall,J., Ohan,V., Pollard,M.O., Whitwham,A., Keane,T., McCarthy,S.A., Davies,R.M., *et al.* (2021) Twelve years of SAMtools and BCFtools. *GigaScience*, **10**, 1–4.
48. Ramírez,F., Ryan,D.P., Grüning,B., Bhardwaj,V., Kilpert,F., Richter,A.S., Heyne,S., Dündar,F. and Manke,T. (2016) deepTools2: a next generation web server for deep-sequencing data analysis. *Nucleic Acids Res.*, **44**, W160–W165.
49. Quadrana,L., Bortolini Silveira,A., Mayhew,G.F., LeBlanc,C., Martienssen,R.A., Jeddeloh,J.A. and Colot,V. (2016) The Arabidopsis thaliana mobilome and its impact at the species level. *eLife*, **5**, e15716.
50. Zhang,Y., Liu,T., Meyer,C.A., Eeckhoute,J., Johnson,D.S., Bernstein,B.E., Nusbaum,C., Myers,R.M., Brown,M., Li,W., *et al.* (2008) Model-based analysis of ChIP-Seq (MACS). *Genome Biol.*, **9**, R137.
51. Pfab,A., Antosz,W., Holzinger,P., Bruckmann,A., Griesenbeck,J. and Grasser,K.D. (2017) Analysis of *in vivo* chromatin and protein interactions of *Arabidopsis* transcript elongation factors. *Methods Mol. Biol.*, **1629**, 105–122.
52. Ewels,P., Magnusson,M., Lundin,S. and Käller,M. (2016) MultiQC: summarize analysis results for multiple tools and samples in a single report. *Bioinformatics*, **32**, 3047–3048.
53. Dobin,A., Davis,C.A., Schlesinger,F., Drenkow,J., Zaleski,C., Jha,S., Batut,P., Chaisson,M. and Gingeras,T.R. (2013) STAR: ultrafast universal RNA-seq aligner. *Bioinformatics*, **29**, 15–21.
54. Okonechnikov,K., Conesa,A. and García-Alcalde,F. (2016) Qualimap 2: advanced multi-sample quality control for high-throughput sequencing data. *Bioinformatics*, **32**, 292–294.
55. Liao,Y., Smyth,G.K. and Shi,W. (2014) featureCounts: an efficient general purpose program for assigning sequence reads to genomic features. *Bioinformatics*, **30**, 923–930.
56. Love,M.L., Huber,W. and Anders,S. (2014) Moderated estimation of fold change and dispersion for RNA-seq data with DESeq2. *Genome Biol.*, **15**, 550.
57. Haag,J.R. and Pikaard,C.S. (2011) Multisubunit RNA polymerases IV and V: purveyors of non-coding RNA for plant gene silencing. *Nat. Rev. Mol. Cell Biol.*, **12**, 483–492.
58. Zhu,J., Liu,M., Liu,X. and Dong,Z. (2018) RNA polymerase II activity revealed by GRO-seq and pNET-seq in *Arabidopsis*. *Nat. Plants*, **4**, 1112–1123.
59. Szádeczky-Kardoss,I., Szaker,H.M., Verma,R., Darkó,É., Pettkó-Szandtner,A., Silhavy,D. and Csorba,T. (2022) Elongation factor TFIIS is essential for heat stress adaptation in plants. *Nucleic Acids Res.*, **50**, 1927–1950.
60. Dhaliwal,N.K. and Mitchell,J.A. (2016) Nuclear RNA Isolation and Sequencing. *Methods Mol. Biol.*, **1402**, 63–71.

61. Zaghlool,A., Ameur,A., Nyberg,L., Halvardson,J., Grabherr,M., Cavelier,L. and Feuk,L. (2013) Efficient cellular fractionation improves RNA sequencing analysis of mature and nascent transcripts from human tissues. *BMC Biotechnol.*, **13**, 99.
62. Yu,X., Martin,P.G.P. and Michaels,S.D. (2019) BORDER proteins protect expression of neighboring genes by promoting 3' Pol II pausing in plants. *Nat. Commun.*, **10**, 4359.
63. Mieczkowski,J., Cook,A., Bowman,S.K., Mueller,B., Alver,B.H., Kundu,S., Deaton,A.M., Urban,J.A., Larschan,E., Park,P.J., *et al.* (2016) MNase titration reveals differences between nucleosome occupancy and chromatin accessibility. *Nat. Commun.*, **7**, 11485.
64. Zhang,T., Zhang,W. and Jiang,J. (2015) Genome-wide nucleosome occupancy and positioning and their impact on gene expression and evolution in plants. *Plant Physiol.*, **168**, 1406–1416.
65. Li,G., Liu,S., Wang,J., He,J., Huang,H., Zhang,Y. and Xu,L. (2014) ISWI proteins participate in the genome-wide nucleosome distribution in *Arabidopsis*. *Plant J.*, **78**, 706–714.
66. Cortijo,S., Charoensawan,V., Brestovitsky,A., Buning,R., Ravarani,C., Rhodes,D., van Noort,J., Jaeger,K.E. and Wigge,P.A. (2017) Transcriptional regulation of the ambient temperature response by H2A.Z nucleosomes and HSF1 transcription factors in Arabidopsis. *Mol. Plant*, **10**, 1258–1273.
67. Piovesan,A., Caracausi,M., Antonaros,F., Pelleri,M.C. and Vitale,L. (2016) GeneBase 1.1: a tool to summarize data from NCBI gene datasets and its application to an update of human gene statistics. *Database*, **2016**, 1–13.
68. Derelle,E., Ferraz,C., Rombauts,S., Rouzé,P., Worden,A.Z., Robbens,S., Partensky,F., Degroeve,S., Echeynié,S., Cooke,R., *et al.* (2006) Genome analysis of the smallest free-living eukaryote *Ostreococcus tauri* unveils many unique features. *Proc. Natl. Acad. Sci. USA*, **103**, 11647–11652.
69. Markusch,H., Michl-Holzinger,P., Obermeyer,S., Thorbecke,C., Bruckmann,A., Babl,S., Längst,G., Osakabe,A., Berger,F. and Grasser,K.D. (2023) ELF1 is a component of the Arabidopsis RNA polymerase II elongation complex and associates with a subset of transcribed genes. *New Phytol.*, **238**, 113–124.
70. Ehara,H., Kujirai,T., Fujino,Y., Shirouzu,M., Kurumizaka,H. and Sekine,S.-I. (2019) Structural insight into nucleosome transcription by RNA polymerase II with elongation factors. *Science*, **363**, 744–747.
71. Rahl,P.B., Lin,C.Y., Seila,A.C., Flynn,R.A., McCuine,S., Burge,C.B., Sharp,P.A. and Young,R.A. (2010) c-Myc regulates transcriptional pause release. *Cell*, **141**, 432–445.
72. Core,L. and Adelman,K. (2019) Promoter-proximal pausing of RNA polymerase II: a nexus of gene regulation. *Genes Dev.*, **33**, 960–982.
73. Rossi,M.J., Kuntala,P.K., Lai,W.K.M., Yamada,N., Badjatia,N., Mittal,C., Kuzu,G., Bocklund,K., Farrell,N.P., Blanda,T.R., *et al.* (2021) A high-resolution protein architecture of the budding yeast genome. *Nature*, **592**, 309–314.
74. Mayer,A., Lidschreiber,M., Siebert,M., Leike,K., Söding,J. and Cramer,P. (2010) Uniform transitions of the general RNA polymerase II transcription complex. *Nat. Struct. Mol. Biol.*, **17**, 1272–1278.
75. Cortazar,M.A., Sheridan,R.M., Erickson,B., Fong,N., Glover-Cutter,K., Brannan,K. and Bentley,D.L. (2019) Control of RNA Pol II speed by PNUTS-PP1 and Spt5 dephosphorylation facilitates termination by a "Sitting Duck Torpedo" mechanism. *Mol. Cell*, **76**, 896–908.
76. Hu,S., Peng,L., Xu,C., Wang,Z., Song,A. and Chen,F.X. (2021) SPT5 stabilizes RNA polymerase II, orchestrates transcription cycles, and maintains the enhancer landscape. *Mol. Cell*, **81**, 4425–4439.
77. Quan,T.K. and Hartzog,G.A. (2010) Histone H3K4 and K36 methylation, Chd1 and Rpd3S oppose the functions of *Saccharomycescerevisiae* Spt4-Spt5 in transcription. *Genetics*, **184**, 321–334.
78. Wada,T., Takagi,G., Yamaguchi,Y., Ferdous,A., Imai,T., Hirose,S., Sugimoto,S., Yano,K., Hartzog,G.A., Winston,F., *et al.* (1998) DSIF, a novel transcription elongation factor that regulates RNA polymerase II processivity, is composed of human Spt4 and Spt5 homologs. *Genes Dev.*, **12**, 343–356.
79. Ehara,H., Yokoyama,T., Shigematsu,H., Yokoyama,S., Shirouzu,M. and Sekine,S.I. (2017) Structure of the complete elongation complex of RNA polymerase II with basal factors. *Science*, **357**, 921–924.
80. Ehrensberger,A.H., Kelly,G.P. and Svejstrup,J.Q. (2013) Mechanistic interpretation of promoter-proximal peaks and RNAPII density maps. *Cell*, **154**, 713–715.
81. Diamant,G., Bahat,A. and Dikstein,R. (2016) The elongation factor Spt5 facilitates transcription initiation for rapid induction of inflammatory-response genes. *Nat. Commun.*, **7**, 11547.
82. Yang,Y., Li,W., Hoque,M., Hou,L., Shen,S., Tian,B. and Dynlacht,B.D. (2016) PAF complex plays novel subunit-specific roles in alternative cleavage and polyadenylation. *PLoS Genet.*, **12**, e1005794.
83. Kim,J., Guermah,M. and Roeder,R.G. (2010) The human PAF1 complex acts in chromatin transcription elongation both independently and cooperatively with SII/TFIIS. *Cell*, **140**, 491–503.
84. Hou,L., Wang,Y., Liu,Y., Zhang,N., Shamovsky,I., Nudler,E., Tian,B. and Dynlacht,B.D. (2019) Paf1C regulates RNA polymerase II progression by modulating elongation rate. *Proc. Natl. Acad. Sci. U.S.A.*, **116**, 14583–14592.
85. van den Heuvel,D., Spruijt,C.G., González-Prieto,R., Kragten,A., Paulsen,M.T., Zhou,D., Wu,H., Apelt,K., van der Weegen,Y., Yang,K., *et al.* (2021) A CSB-PAF1C axis restores processive transcription elongation after DNA damage repair. *Nat. Commun.*, **12**, 1342.
86. Vos,S.M., Farnung,L., Boehning,M., Wigge,C., Linden,A., Urlaub,H. and Cramer,P. (2018) Structure of activated transcription complex Pol II-DSIF-PAF-SPT6. *Nature*, **560**, 607–612.
87. Tellier,M., Maudlin,I. and Murphy,S. (2020) Transcription and splicing: a two-way street. *WIREs RNA*, **11**, e1593.
88. Giono,L.E. and Kornblihtt,A.R. (2020) Linking transcription, RNA polymerase II elongation and alternative splicing. *Biochem. J.*, **477**, 3091–3104.
89. Marquardt,S., Petrillo,E. and Manavella,P.A. (2023) Cotranscriptional RNA processing and modification in plants. *Plant Cell*, **35**, 1654–1670.
90. Godoy Herz,M.A. and Kornblihtt,A.R. (2019) Alternative splicing and transcription elongation in plants. *Front. Plant Sci.*, **10**, 309.
91. Koncz,C., Dejong,F., Villacorta,N., Szakonyi,D. and Koncz,Z. (2012) The spliceosome-activating complex: molecular mechanisms underlying the function of a pleiotropic regulator. *Front. Plant Sci.*, **3**, 9.
92. Li,Y., Yang,J., Shang,X., Lv,W., Xia,C., Wang,C., Feng,J., Cao,Y., He,H., Li,L., *et al.* (2019) SKIP regulates environmental fitness and floral transition by forming two distinct complexes in Arabidopsis. *New Phytol.*, **224**, 321–335.
93. Tettey,T.T., Gao,X., Shao,W., Li,H., Story,B.A., Chitsazan,A.D., Glaser,R.L., Goode,Z.H., Seidel,C.W., Conaway,R.C., *et al.* (2019) A role for FACT in RNA polymerase II promoter-proximal pausing. *Cell Rep.*, **27**, 3770–3779.
94. Martin,B.J.E., Chruscicki,A.T. and Howe,L.J. (2018) Transcription promotes the interaction of the FAcilitates Chromatin Transactions (FACT) complex with nucleosomes in *Saccharomyces cerevisiae*. *Genetics*, **210**, 869–881.
95. Jeronimo,C., Angel,A., Nguyen,V.Q., Kim,J.M., Poitras,C., Lambert,E., Collin,P., Mellor,J., Wu,C. and Robert,F. (2021) FACT is recruited to the +1 nucleosome of transcribed genes and spreads in a Chd1-dependent manner. *Mol. Cell*, **81**, 3542–3559.
96. Vinayachandran,V., Reja,R., Rossi,M.J., Park,B., Rieber,L., Mittal,C., Mahony,S. and Pugh,B.F. (2018) Widespread and

precise reprogramming of yeast protein-genome interactions in response to heat shock. *Genome Res.*, **28**, 357–366.
97. Ehara,H., Kujirai,T., Shirouzu,M., Kurumizaka,H. and Sekine,S.-I. (2022) Structural basis of nucleosome disassembly and reassembly by RNAPII elongation complex with FACT. *Science*, **377**, eabp9466.
98. Farnung,L., Ochmann,M., Engeholm,M. and Cramer,P. (2021) Structural basis of nucleosome transcription mediated by Chd1 and FACT. *Nat. Struct. Mol. Biol.*, **28**, 382–387.
99. Liu,M., Zhu,J. and Dong,Z. (2021) Immediate transcriptional responses of Arabidopsis leaves to heat shock. *J.Integr.Plant Biol*, **63**, 468–483.
100. Kindgren,P., Ivanov,M. and Marquardt,S. (2020) Native elongation transcript sequencing reveals temperature dependent dynamics of nascent RNAPII transcription in Arabidopsis. *Nucleic Acids Res.*, **48**, 2332–2347.
101. Mylonas,C. and Tessarz,P. (2018) Transcriptional repression by FACT is linked to regulation of chromatin accessibility at the promoter of ES cells. *Life Sci. Alliance*, **1**, e201800085.
102. Brahma,S. and Henikoff,S. (2020) Epigenome regulation by dynamic nucleosome unwrapping. *Trends Biochem. Sci.*, **45**, 13–26.
103. Lai,W.K.M. and Pugh,B.F. (2017) Understanding nucleosome dynamics and their links to gene expression and DNA replication. *Nat. Rev. Mol. Cell Biol.*, **18**, 548–562.

Received: April 14, 2023. **Revised:** August 24, 2023. **Editorial Decision:** September 18, 2023. **Accepted:** September 21, 2023